

Etched Colloidal LiFePO₄ Nanoplatelets Toward High-Rate Capable Li-ion Battery Electrodes

Andrea Paolella^{1,2,†}, Giovanni Bertoni^{1,3,†}, Sergio Marras^{1,†}, Enrico Dilella¹, Massimo Colombo¹, Mirko Prato¹, Andreas Riedinger^{1,4}, Mauro Povia¹, Alberto Ansaldo¹, Karim Zaghib², Liberato Manna^{1}, and Chandramohan George^{1,5*}*

¹Nanochemistry Department, Istituto Italiano di Tecnologia, Via Morego 30, 16163 Genova, Italy

²Institut de recherche d'Hydro-Québec (IREQ), 1800 Boulevard Lionel Boulet, Varennes, QC, J3X1S1, Canada

³IMEM-CNR, Parco Area delle Scienze 37/A, 43124 Parma, Italy

⁴Optical Materials Engineering Laboratory, ETH Zurich, 8092 Zurich, Switzerland

⁵Institute for Manufacturing, Department of Engineering, 17 Charles Babbage Road, University of Cambridge, CB3 0FS, United Kingdom

[†] **A.P., G.B. and S.M. equally contributed to this work**

KEYWORDS: Nanocrystals, platelet-shape, LiFePO₄, Li-ion batteries, rate performance

* gc495@cam.ac.uk; liberato.manna@iit.it

Supporting information

Chemicals.

Oleylamine (OAm, 70% purum), 1-octadecene (technical grade, 90%), iron (II) chloride anhydrous (99.99% purum), ammonium phosphate dibasic ($\geq 99.99\%$ purum), lithium iodide (beads, $\geq 99.99\%$ purum), α -D-glucose (96 % purum, anhydrous), electrochemical grade propylene carbonate, ethylene carbonate, diethyl carbonate, N-methyl-2-pyrrolidone, (poly) and vinylidene difluoride were purchased from Sigma Aldrich. Chloroform and ethanol were purchased from Carlo Erba. Coin type 2032 components (SS casing items) were purchased from Hohsen Corporation. Polypropylene (PP) microporous films were purchased from Cellguard. Carbon powder (carbon super P) was purchased from Alfa Aesar. Pure Li metal foils were purchased from Goodfellow.

X-ray photoelectron spectroscopy (XPS) and Electron Energy Loss Spectroscopy (EELS) Quantification

The platelets were analyzed by X-ray photoelectron spectroscopy (XPS). Our data are in good agreement with those reported for 100 nm diameter LiFePO_4 nanoparticles¹. The particular shape of the Fe 2p spectrum, due to multiple splitting,¹ together with the position of the Fe 3p peak at 55.3 eV, is a confirmation that the oxidation state of Fe is +II. The P 2p spectrum can be easily decomposed in two spin-orbit components at 133.3 eV and 134.2 eV. These positions, together with the position of the O 1s peak at 531.4 eV, are in good agreement with the presence of $(\text{PO}_4)^{3-}$ groups.²

Li ions can be detected by Electron Energy Loss Spectroscopy (EELS) in the electron microscope, by quantifying the ratio between the Li-K ionization edge intensity (~ 55 eV) and the Fe-L ionization edge (~ 708 eV), using model based techniques.³ Unfortunately, the Li-K edge and Fe- $M_{2,3}$ edge have onsets at similar energies (~ 55 eV and ~ 54 eV respectively, according to the EELS reference database from Gatan Inc.). Figure S3 illustrates the problem, showing the models used for the Li-K (blue line) and Fe-M (red line) ionization edges. To separate the two signals we verified the spectral intensity of the Fe- $M_{2,3}$ edge with respect to the Fe- $L_{2,3}$ edge (the last one usually used for quantification), by acquiring the spectra at the same conditions on a Fe_2O_3 reference sample (from Aldrich Inc.). The intensity of the Fe- $M_{2,3}$ edge was then kept fixed to the ratio measured from the reference sample. The amount of signal left in the spectrum in the region 50-130 eV was then fitted with a Li-K cross section (see Figure S4). The quantification was performed using the model based technique as in EELSMODEL, and adding an

equalization function mimicking the density of states (DOS).⁴ Despite model-based quantification can give very accurate and precise results in case of Poisson statistics, in our case the precision of the fits is lowered by the high background level in the spectra at low energy loss. We found that a log-polynomial function better describes the background of the spectra in the low-energy range with respect to the power-law function. The precision in the estimated amounts was around 10% for Fe, O, and P, and around 20% for Li, respectively. Figure S4 shows the results of model-based fitting on the different elements. As a result, we obtained a Li/Fe ratio of 0.7 (± 0.2), a P/Fe ratio of 0.9 (± 0.1) and O/Fe ratio of 3.8 (± 0.4), close to the expected stoichiometry of LiFePO_4 .

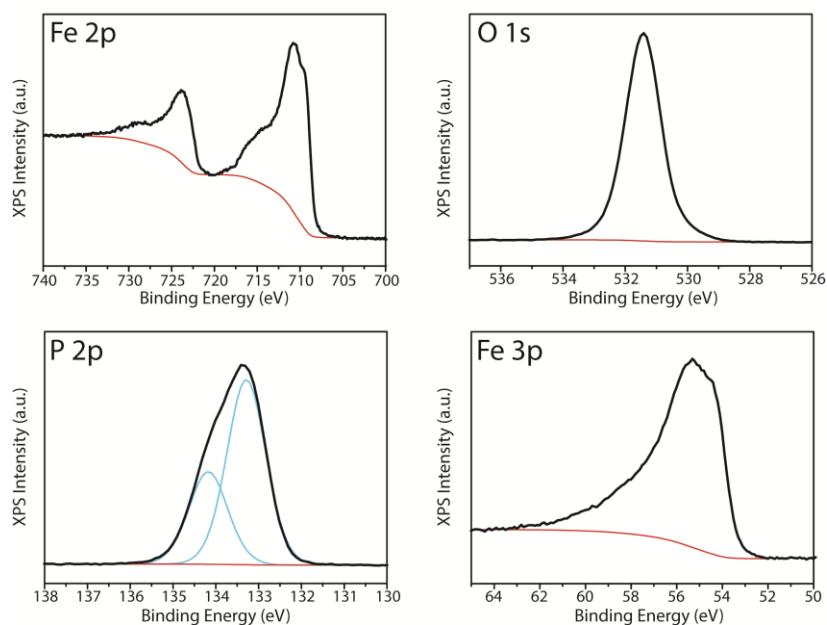


Figure S1 High resolution XPS spectra narrow scans on Fe 2p, O 1s, P 2p and Fe 3p binding energy ranges. Experimental data (black lines) are shown together with Shirley-type backgrounds (red lines). Deconvolution of the P 2p doublet using Gauss-Lorentz profiles is also shown. Note that the Li 1s peak (usually found at approx. 55 eV) is buried in the intense Fe 3p peak since, in our experimental conditions, its relative sensitivity factor is about 15 times smaller than that of Fe 3p.

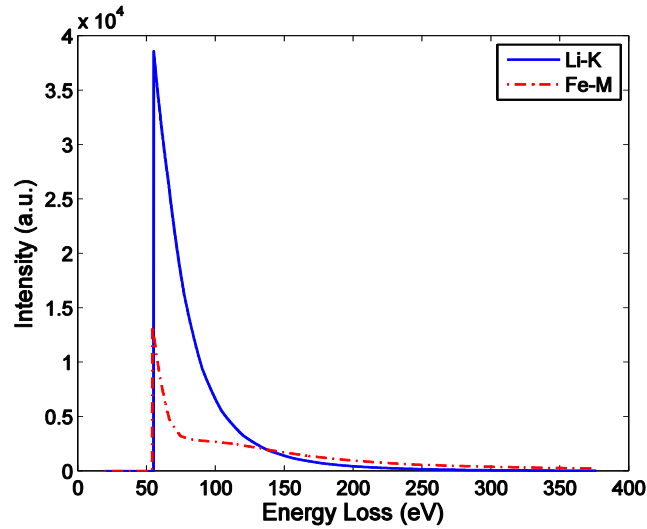


Figure S2. Comparison of the relative intensities of the Li-K ionization edge and the Fe-M_{2,3} ionization edge, calculated using Hartree-Slater parameterized cross sections, at $E_0 = 200$ kV incident energy, $\alpha = 1.5$ mrad, and $\beta = 5.0$ mrad as in the experimental conditions.

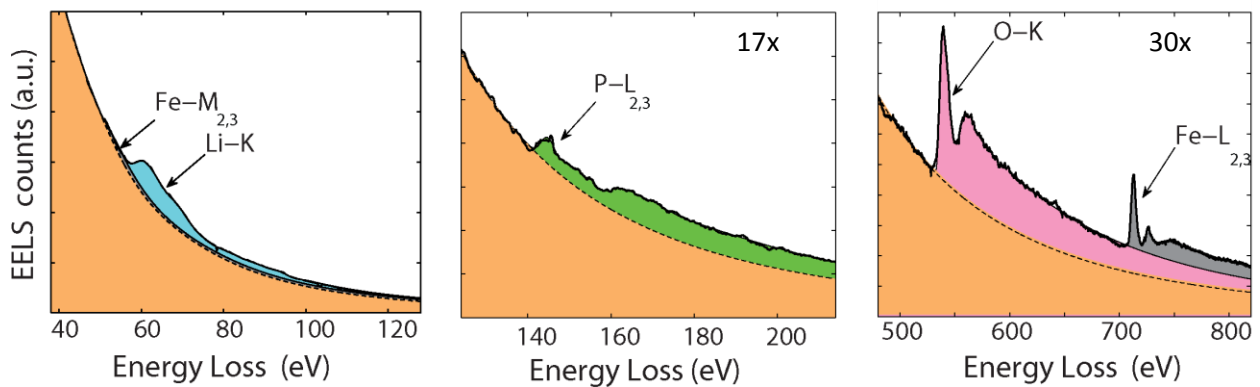


Figure S3. The results of model based EELS fits of the Li-K, the P-L_{2,3}, the O-K and Fe-L_{2,3} edges, respectively. The Li-K cross section is multiplied by a DOS function. Note the high background in the spectrum from Li-K, making a precise quantification of the Li amount a difficult task.

^{19}F -NMR spectrum LiFePO_4 before and after etching

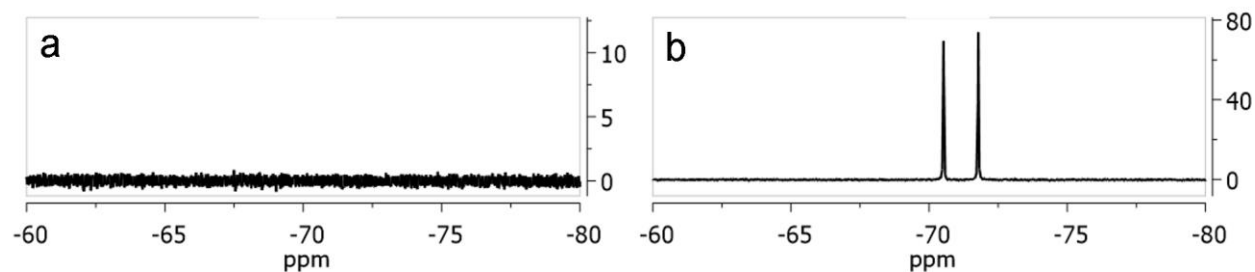


Figure S4: a) ^{19}F -NMR spectrum from a solution of the as-synthesized NCs(a) and etched NCs (b). No PF_6^- could be detected in the spectrum a) while in b) the presence of PF_6^- is confirmed by the characteristic doublet at -70.5 and 71.8 ppm.⁵

XRD analysis of LFP nanoplatelets after PF_6^- treatment and after carbon coating

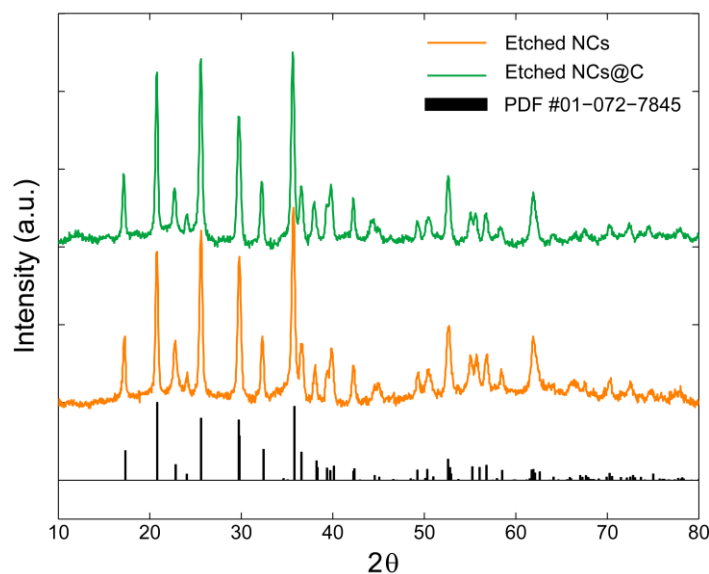


Figure S5: XRD patterns of the etched NCs (after PF_6^- treatment - orange line) and etched NCs @C (after PF_6^- treatment and carbon coating - green line). They are both consistent with olivine-type LiFePO_4 (PDF card number 01 - 072 - 7845).

Thermogravimetric analysis (TGA) on as-synthesized and etched NCs

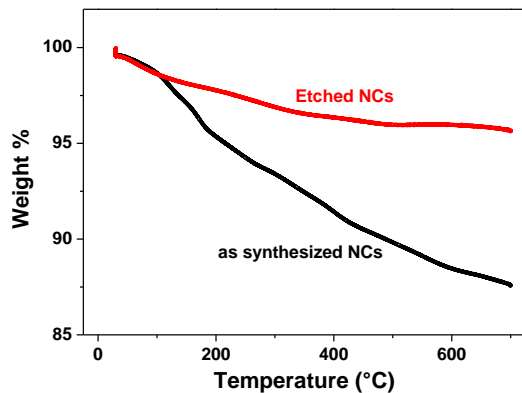


Figure S6 Thermogravimetric analysis (TGA) of the as-synthesized NCs (black curve) and etched NCs (red curve).

TEM imaging of etched and carbon coated samples

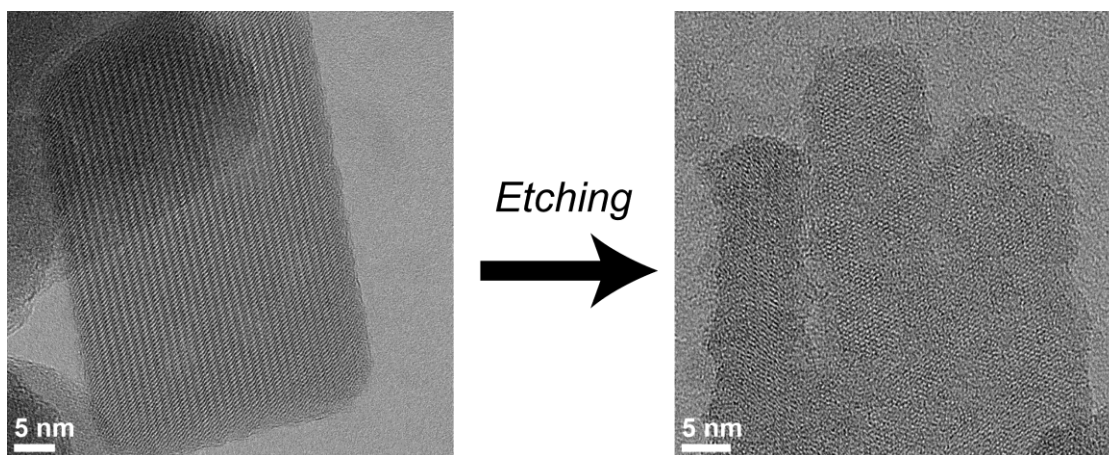


Figure S7. TEM images of LiFePO_4 platelets before and after etching (statistics from HRTEM images showed an increase in roughness from 0.5 ± 0.1 nm to 0.9 ± 0.1 nm).

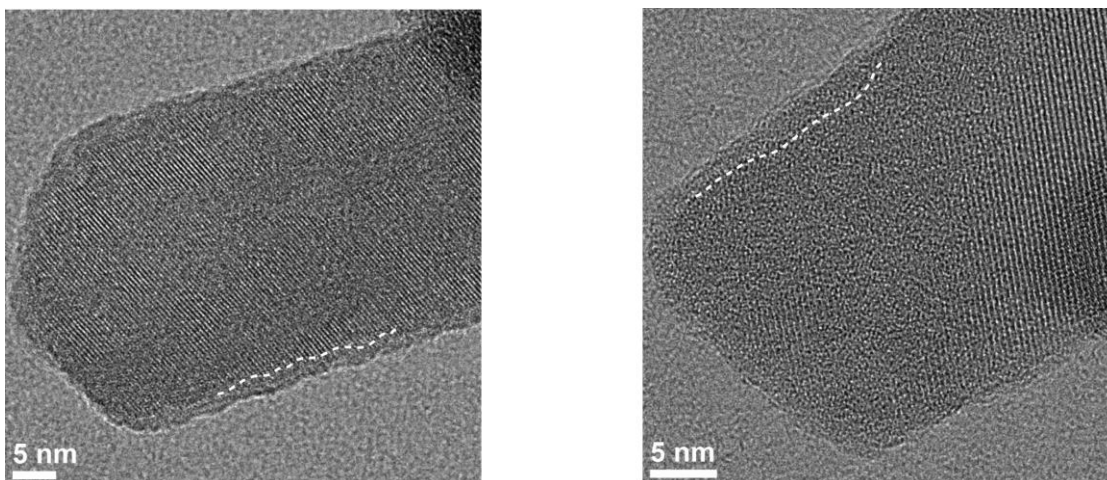


Figure S8. TEM analysis of the etched NCs@C evidencing their roughened surface after etching and carbon coating.

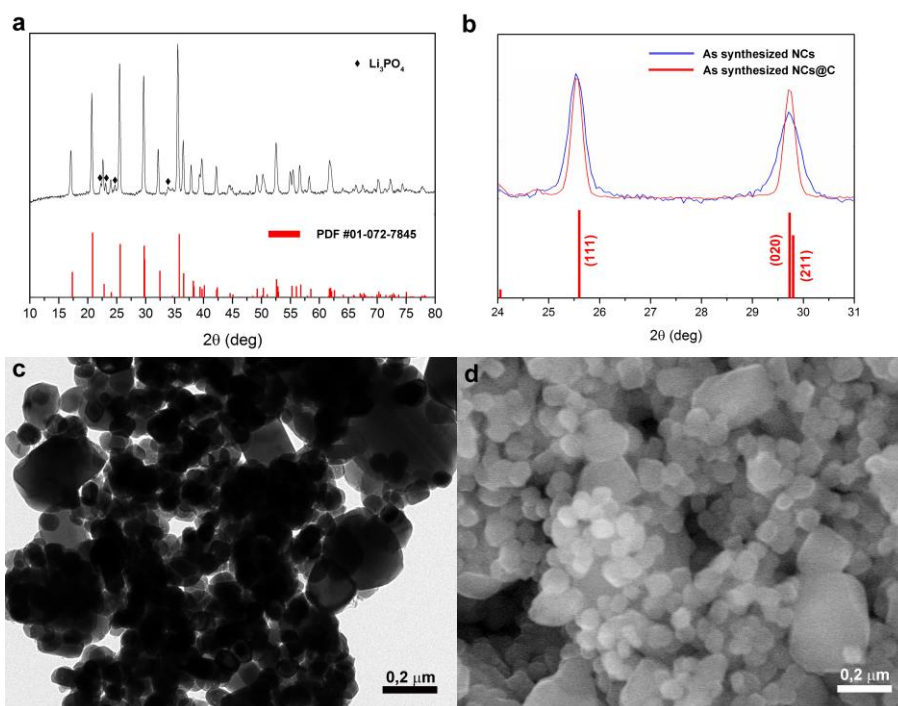


Figure S9 a) XRD pattern of as synthesized NCs@C showing the presence of Li_3PO_4 impurity, b) magnification of low angle part of the XRD pattern displayed in a) for the sample before (blue line) and after carbon coating (red line), c) TEM and d) SEM. images of the as synthesized NCs@C showing the formation of large crystals, due coalescence effects during the carbon coating process,

Brunauer–Emmett– Teller (BET) surface area results

Sample	BET Surface Area (m ² /g)
As-synthesized NCs	57.0
As-synthesized NCs@C	22.8
Etched NCs	70.5
Etched NCs@C	52.1

Table T1. BET Specific surface areas of LPF NCs

Additional details on electrodes prepared from as synthesized LiFePO₄ NCs etched LiFePO₄ NCs and carbon coated LiFePO₄ NCs

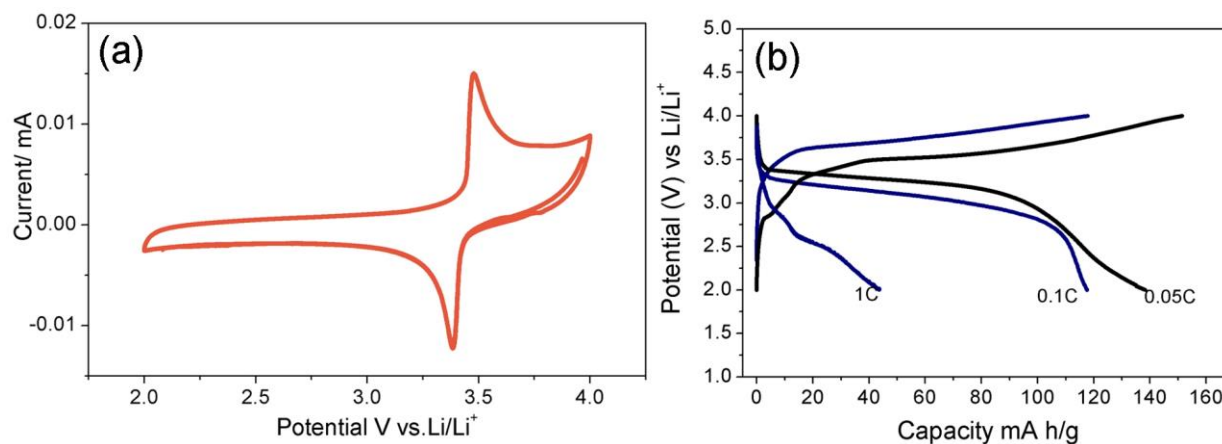


Figure S10 a) Cyclic voltammetry (CV) of the as-synthesized NCs (with oleylamine as surfactant) electrodes performed at 0.1 mV/s); c) charge/discharge cycles of the as-synthesized NCs electrode at 0.05 C, at 0.1 C and 1 C.

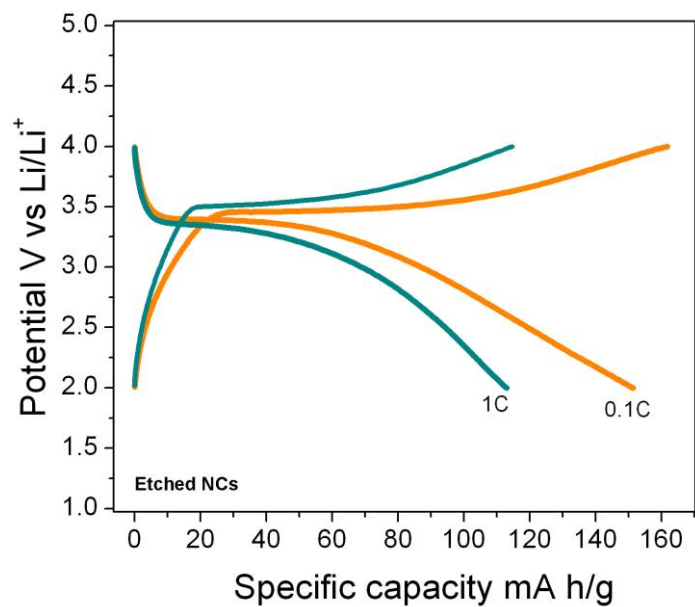


Figure S11 Charge/discharge cycles of the etched NCs electrode at 0.1 C and at 1 C.

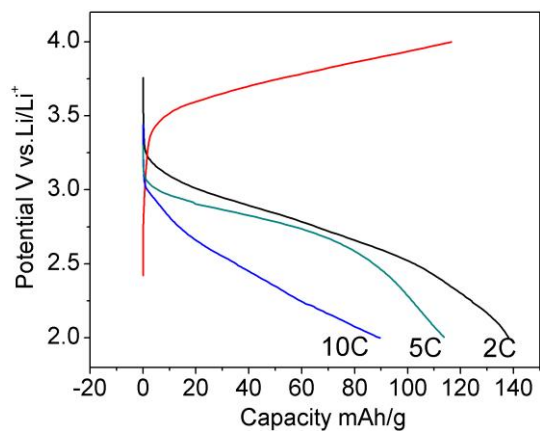


Figure S12: a) Charge/discharge cycles of the as-synthesized NCs@C (non-etched carbon coated) at 2C, 5C and 10C.

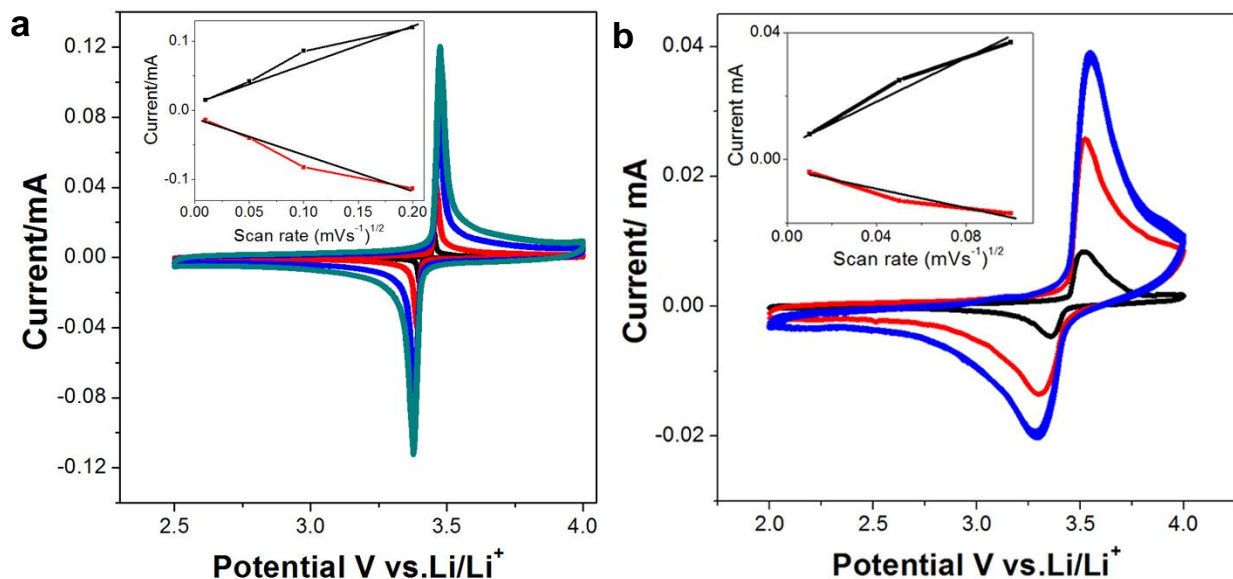


Figure S13: The linear plots of I_{pc} vs $v^{1/2}$ for a) etched NCs@C samples and b) as synthesized NCs@C. Li ion diffusion coefficient using Randles-Sevcik equation; $I_{pc}=2.69 \times 10^5 n^{3/2} AD^{1/2} C v^{1/2}$, where I_{pc} is peak current (amperes), n is the number of electrons involved in the metal redox center (Fe^{2+}/Fe^{3+}), A is specific surface area obtained from BET data (cm^2), D is the Li ion diffusion coefficient in $LiFePO_4$ ($cm^2 s^{-1}$), C is the molar concentration of Li ions in $LiFePO_4$ and v is the scan rate used in the CV (Vs^{-1}).

References

1. Grosvenor, A.P., Kobe, B.A., Biesinger, M.C. & McIntyre, N.S. Investigation of multiplet splitting of Fe 2p XPS spectra and bonding in iron compounds. *Surface and Interface Analysis* **36**, 1564-1574 (2004).
2. Dedryvere, R. et al. X-Ray Photoelectron Spectroscopy Investigations of Carbon-Coated Li_xFePO_4 Materials. *Chemistry of Materials* **20**, 7164-7170 (2008).
3. Bertoni, G. & Verbeeck, J. Accuracy and precision in model based EELS quantification. *Ultramicroscopy* **108**, 782-790 (2008).
4. Verbeeck, J., Van Aert, S. & Bertoni, G. Model-based quantification of EELS spectra: Including the fine structure. *Ultramicroscopy* **106**, 976-980 (2006).
5. Ciancaleoni, G., Zuccaccia, C., Zuccaccia, D. & Macchioni, A. Diffusion and NOE NMR studies on the interactions of neutral amino-acidate arene ruthenium(II) supramolecular aggregates with ions and ion pairs. *Magnetic Resonance in Chemistry* **46**, S72-S79 (2008).